Hydrogen Bonds Dictate O₂ Capture and Release within a Zinc Tripod

Eric W. Dahl[#,a], **John J. Kiernicki**[#,a], **Matthias Zeller**[b], and **Nathaniel K. Szymczak**[*,a]

[a]Department of Chemistry, University of Michigan, 930 N. University Ave., Ann Arbor, MI 48109.

[b]H. C. Brown Laboratory, Department of Chemistry, Purdue University, West Lafayette, IN 44555.

[#] These authors contributed equally to this work.

Abstract

Six directed hydrogen bonding (H-bonding) interactions allow for the reversible capture and reduction of dioxygen to a *trans*-1,2-peroxo within a tripodal zinc(II) framework. Spectroscopic studies of the dizinc peroxides, as well as on model zinc diazides, suggest H-bonding contributions serve a dominant role for the binding/activation of these small molecules.

Abstract
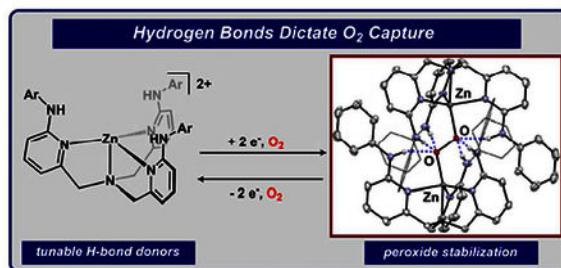
The reversible capture of dioxygen as peroxide (O_2^{2-}) is required for myriad biological and abiological reactions spanning from oxidases to metal-air batteries.[1] Biological systems leverage well-positioned secondary coordination sphere interactions, such as hydrogen bonding (H-bonding), within their active metal site(s) to achieve selective O₂ binding, activation, and transfer.[2] To emulate this principle, recent synthetic systems have demonstrated that H-bonds can facilitate O₂ capture in the superoxo or peroxo state, although binding is typically coupled with a metal-based redox event.[3] In contrast, capture of the O₂ unit using H-bonds as the primary binding interaction is very rare,[4] and was recently enabled by six directed H-bonds within a cryptand-type macrocycle.[5] In this case, O₂ capture was facilitated by preorganization of a molecular capsule with a binding pocket size-matched for a diatom. Given that host/guest inclusion is highly sensitive to size

complementarity,[6] the use of a preassembled binding pocket complicates the role that the H-bonds serve in capture and/or stabilization. An open tripodal ligand provides one test of whether preassembly is required to capture O_2 using H-bonds without a redox-active metal.

Our group is working to evaluate how the precise structural, electronic, and cooperative modes in the secondary coordination sphere can be used to regulate reactivity.[7] Recently, we reported a family of *p*-substituted tris(6-(*p*-R-phenylamino-2-pyridylmethyl)amine ligands (L^R, R = CF_3, H, OMe) that provide electronically tunable −NHAr H-bond donors in the secondary coordination sphere.[7f] This ligand framework provided the first structural characterization of an H-bonded (*trans*-1,2-peroxo)dicopper complex in which a combination of six H-bonds and two Cu(II) centers encapsulate the O_2^{2-} unit. We hypothesized that if the six H-bonds to peroxide were key factors that allowed isolation, then the templating metal and the reductant could be separated. Zinc(II), the ubiquitous redox-inactive d-block metal, was selected to test this hypothesis (Fig. 1). Tripodal ligand scaffolds containing H-bond donors within the secondary coordination sphere have been recently popularized[8] and have previously been templated on zinc.[9] Zn_2O_2 fragments remain exceedingly rare and are limited to polymetallic aggregates with greater than two metals.[10] Herein, we report dioxygen capture and reduction enabled by H-bonds via (*trans*-1,2-peroxo)dizinc complexes as well as the reverse—dioxygen release.

An H-bonded dizinc peroxide was obtained from dioxygen and reductant in the presence of $[ZnL^H]^{2+}$. Saturation of an equimolar MeCN solution of L^H and $Zn(OTf)_2$ with O_2 followed by rapid addition of bis(cyclopentadienyl)cobalt(II) at room-temperature afforded the (*trans*-1,2-peroxo)dizinc complex, $[(L^H)_2 Zn_2 O_2][OTf]_2$ ($\mathbf{1^H}$), in 89% yield (Fig. 2).[11] An alternative synthesis of $\mathbf{1^H}$ was also developed: sequential addition of H_2O_2 and N^iPr_2Et to a MeCN solution of L^H and $Zn(OTf)_2$ afforded $\mathbf{1^H}$ in 58% yield.[12–13] $\mathbf{1^H}$ is thermally stable in CD_3CN for >18 h at 50 °C in an inert atmosphere and is also moisture tolerant.[14] However, the addition of a competitive H-bond acceptor (i.e. chloride) induces degradation.[15]

The structural metrics of $\mathbf{1^H}$ were elucidated by single-crystal X-ray diffraction (XRD) and revealed a *trans*-1,2-peroxo binding mode with six directed H-bonds to the O_2^{2-} fragment, establishing the first example of a discrete (*trans*-1,2-peroxo)dizinc species. For each '(L^R)Zn' fragment, one −NHPh group engages in H-bonding interactions with the proximal oxygen (N-$O_{proximal}$ = 2.738 Å; N-H-O = 158.97°) while two engage the distal oxygen (N-O_{distal} = 2.837 Å (for both); N-H-O = 176.16 and 169.98°). The N-O distances and N-H-O angles are consistent with moderate-strength H-bonding interactions.[16] The N-C_{pyr} distances range 1.3587(14)-1.3675(14) Å and are consistent with single-bonds where the N-H has not been deprotonated.[17] The O_2 motif (O1-O1' = 1.4954(13) Å) is more reduced than dioxygen[18] or superoxide,[19] and comparable to main-group *trans*-1,2-peroxides including $[O_2 (B(C_6 F_5)_3)_2]^{2-}$ (1.488 Å)[20] and $L_2B_2O_2$ [21] (1.484 Å; L = subporphyrin).[22] Notably, the O-O distance is the same as isostructural $[(L^H)_2 Cu_2O_2]^{2+}$ (1.477(5) Å), which suggests that the ligand scaffold itself may serve a key role in regulating the structure, rather than the metal.

To interrogate the requirement of H-bonding for peroxide capture, we evaluated an isosteric ligand variant, tris(6-phenoxy-2-pyridylmethyl)amine (TPA^{OPh}), that does not contain H-

bond donors. In contrast to L^H, when TPA^{OPh} and $Zn(OTf)_2$ were combined and treated with H_2O_2 and $^iPr_2NEt$, we observed demetalation, rather than the formation of a (*trans*-1,2-peroxo)dizinc (see SI). Attempts to synthesize the zinc analogue of Karlin's $[(TPA)_2 Cu_2 O_2]^{2+}$ (TPA = tris(2-methylpyridylamine)[23] resulted in products derived from $[(TPA)Zn(OH)]^+$.[24–25] These results highlight the synergistic effect of H-bonds with the Zn center in 1^R to both capture and stabilize O_2^{2-}.

Given the role of H-bonds for O_2^{2-} capture, we assessed the extent to which activation of the O–O unit could be tuned by H-bond donor strength. We selected ligand variants that feature identical steric properties surrounding the Zn_2O_2 core, yet vary in acidity of the NH, and thus H-bond donor strength. Given the highly coupled ligand structure, substituent modification will necessarily alter both H-bond donor strength and ligand electronics.[26] For example, an electron-withdrawing aniline (e.g. *p*-CF_3) will afford a better H-bond donor at the expense of a weaker ligand donor strength. Four *para*-substituted anilines with Hammett substituent (σ_p) constants ranging −0.83 (R = NMe_2) to 0.54 (R = CF_3)[27] were used to prepare the series of (*trans*-1,2-peroxo)dizinc complexes (1^R; R = NMe_2, OMe, CF_3; Fig. 2).

The electronic environment provided by each ligand variant in 1^R tracked with the methylene resonances (coupled doublets) of the C_3-symmetric ^1H NMR spectra. For example, electron-deficient 1^{CF3} exhibits the most downfield resonances (4.22 and 4.08 ppm), while the more electron-rich 1^{NMe2} features the most upfield resonances (4.00 and 3.86 ppm). These resonances show a good correlation when plotted against Hammett constants (see SI) and provide a descriptive measure of electronic environment provided by each ligand scaffold. In contrast to the direct relationship between ligand electronic environment and the methylene resonances, the −NH resonance involved in H-bonding interactions, which is a composite of −NH—$O_{proximal}$ and −NH—O_{distal}, does not exhibit the same trend. 1^H displays the most downfield shift (10.21 ppm) while 1^{OMe} and 1^{NMe2} exhibit the same shift (10.14 ppm). The absence of a clear trend contrasts with the previously reported series of $(L^R)CuCl$,[7f] where the −NH resonances exhibit a linear correlation with Hammett constants, and suggests the −NH—O interactions in **1** are not adequately described by simple H-bond donor/acceptor contributions, but may also be influenced by the electronics at zinc.

To probe the origin of the ^1H NMR discrepancies, the structural metrics of 1^R were examined by single-crystal XRD. Complexes 1^{CF3}, 1^{OMe}, and 1^{NMe2} are isostructural to 1^H with six directed H-bonds to the peroxide. The electronic substitutions have negligible consequence on the ability of zinc to dimerize about the O_2^{2-} unit—the Zn-Zn distances range from 4.719 (1^{CF3}) to 4.784 (1^{OMe}) Å. The Zn-O distance reports on the electronic environment of the TPA-ligand: the most electron-deficient variant, 1^{CF3}, displays the shortest Zn-O distance while the most electron-rich variant, 1^{NMe2}, contains the longest (1.9507(16) and 1.991(3) Å, respectively). The H-bonding interactions within the four species are comparable with N-$O_{proximal}$ and N-O_{distal} distances ranging from 2.619–2.741 and 2.811–2.945 Å, respectively.[28] Within the series of complexes, the O–O bond length exhibits a variable extent of activation and ranges from 1.483(6) (1^{NMe2}) to 1.524(3) Å (1^{CF3}). Notably, the O–O bond in 1^R does not correlate with either the electronic character of the TPA-ligand—as assessed by Hammett constants of *para*-aniline substitution—or the

H-bond donor strength. This directly contrasts the $[(L^R)_2Cu_2O_2]^{2+}$ series whose LMCT-energy correlated to TPA-ligand electronics,[7f] further suggesting multiple competing factors contribute to the overall description of the Zn_2O_2 unit.

Oxidation studies were pursued to assess the reversibility of H-bond mediated O_2 capture.[29] Addition of $PhICl_2$ to 1^H cleanly produces $[(L^H)ZnCl][(OTf)]$ (76% yield) concomitant with gas evolution. A Clark electrode was used to confirm O_2 release during oxidation. Because this analytical technique requires aqueous conditions, the reaction was repeated with a water-soluble oxidant. Injection of 1^H into an aqueous solution containing $[NH_4]_2[Ce(NO_3)_6]$ and $[Bu_4N][Cl]$ caused a rapid increase in dissolved O_2, which reached a plateau after 3 minutes, corresponding to approximately 47% yield (Fig. 3, see SI). $[(L^H)ZnCl][(OTf)]$ was formed as the $(L^H)Zn$-containing compound in a similar isolated yield as O_2 (40%).[30] These studies confirm that capture and release is dictated by the direction of electron flow in solutions containing $[(L^H)Zn]^{2+}$.

Azide is a spectroscopic analogue for peroxide due to its similar frontier orbital manifold.[31] In contrast to peroxo-units whose vibrational modes can be challenging to identify,[32] metal-azides feature intense bands that are sensitive to electronic perturbations. We thus sought to interrogate the electronic and H-bonding contributions imparted on the O_2^{2-} or N_3^- unit within a set of isostructural $(L^R)Zn$ complexes.[33] Octahedral $(L^R)Zn(N_3)_2$ complexes (2^R) were targeted because they feature both axial and equatorial azide environments, and only the axial azide can engage in H-bonding interactions. Complexes 2^R were synthesized by treating an acetone solution of L^R and $Zn(ClO_4)_2\cdot6H_2O$ with excess NaN_3 (Fig. 4). The ^1H NMR spectra exhibit downfield −NH resonances, consistent with H-bonding, which are dependent on TPA-ligand electronics. The furthest downfield −N*H* and methylene resonances (δ = 9.36 and 4.16, respectively) correspond to the most electron-deficient variant, 2^{CF3}, while the furthest upfield −NH and methylene resonances (δ = 8.90 and 4.05 ppm respectively), correspond to the most electron-rich complex, 2^{NMe2}.[34] The trend of the −N*H* resonance position contrasts with the series of 1^R (a composite of −NH—$O_{proximal}$ and −NH—O_{distal} interactions) but is analogous to the chloride series, $(L^R)CuCl$.[7f]

Molecular structures for 2^R were determined by single-crystal XRD and establish an octahedral geometry in which the axial azide is engaged in H-bonding to the aniline-NH groups. All three H-bonding interactions are directed to the α-nitrogen of the azide; for 2^{NMe2}, the N_H-N_{azide} distances range 2.919–3.049 Å—consistent with moderate-strength H-bonding interactions.[16] The Zn-$N_{3(equatorial)}$ bond lengths reflect the electronic perturbations of the TPA-ligand (2^{CF3} = 2.063(3); 2^{NMe2} = 2.1357(15) Å); in contrast, minimal variation is displayed within the Zn-$N_{3(axial)}$ bond (2^{CF3} = 2.055(3); 2^{NMe2} = 2.0741(15) Å). Furthermore, the bond distances for the previously reported $(TPA)Zn(E_3)_2$ (E_3 = -N_3[35] or -NCS[36]) compounds are consistent with the equatorial, but *not* axial azide units of 2^R. This disparity suggests that the polarization of the axial azide ligand in 2^R may be governed by H-bonding interactions rather than the overall electronic environment of the TPA-ligand. Vibrational spectroscopy was employed as a complementary metric to decipher azide polarization (similar to gauging CO activation of M-CO species),[37] given the low precision in experimentally determined N—N distances.

The independent impact of H-bonding interactions and electronic character in **2^R** was evident by solid-state IR spectroscopy.[38] Each complex displays two distinct $\nu_{(N3)asymm}$ modes that were identified by DFT analysis as the $\nu_{(N3)}$-equatorial and $\nu_{(N3)}$-axial.[39] In each complex, the H-bonded axial-azide is shifted to higher energy than that of the equatorial azide. Plots of the $\nu_{(N3)}$-equatorial and $\nu_{(N3)}$-axial shift for each complex verses their Hammett substituent constant (Figure 5) exhibit different slopes. The energies of $\nu_{(N3)}$-axial (with H-bonding) are minimally perturbed across the series of complexes (**2^{CF3}** = 2076; **2^{NMe2}** = 2069; Δ = 7 cm^{-1}) as compared to the energies of $\nu_{(N3)}$-equatorial (without H-bonding) (**2^{CF3}** = 2038; **2^{NMe2}** = 2057; Δ = 19 cm^{-1}) and is consistent with the trend in crystallographically determined Zn–N$_{3(equatorial)}$ bond distances. We propose that the H-bonds in **2^R** serve as the primary activating interaction for the axial azide, similar to previously reported (L^{OH})CuF (L^{OH} = tris(6-hydroxy-2-methylpyridyl)amine), where halide (F-) binding was dictated by H-bonds, rather than a Cu(I)-F interaction.[40] By extension, the intramolecular H-bonding interactions in **2^R** attenuate the electronic influence of ligand variation by reducing the covalency between Zn(II) and azide. We propose that this same phenomenon can be applied to rationalize the spectroscopy of **1^R**. The non-linear correlation of the O-O bond distances as well as the ^{1}H NMR $-NH$ resonances, with respect to Hammett constants, both imply the six H-bonding interactions to the O$_2{}^{2-}$ unit play a greater role in substrate activation than the electronic influence of the supporting TPA-ligand acting on the zinc center.

We have demonstrated that an H-bond appended tripodal zinc complex assembles to capture peroxide derived from dioxygen and electrons. This is the first example of a discrete (*trans*-1,2-peroxo)dizinc complex and its isolation was facilitated by H-bonding interactions. The captured peroxide can be liberated as dioxygen via two-electron chemical oxidation. The TPA derivatives, tris(6-(*p*-R-phenylamino-2-pyridylmethyl)amine, provide tunable secondary sphere H-bond donors that augment the stabilization of otherwise unstable Zn$_2$O$_2$ units. Analysis of a series of related zinc-diazide complexes revealed that H-bonding interactions serve as the primary component responsible for substrate capture and activation in the absence of a redox-active metal.

Supplementary Material

Refer to Web version on PubMed Central for supplementary material.

ACKNOWLEDGMENT

REFERENCES

(1). (a)Conte V ; Bortolini O : Z. In The Chemistry of Peroxides, Rappoport Z , Ed; John Wiley & Sons: New York, 2006; Vol. 2, Part 2, pp 1053–1128;(b)Dioxygen Activation and Homogeneous Catalytic Oxidation, 1st ed.; Simandi LI ; Elsevier Science Publishers B.V.: New York, 1991; (c)Metal-Oxo and Metal-Peroxo Species in Catalytic Oxidation. Meunier B ; Springer-Verlag Berlin Heidelberg: 2000;(d)Fu J ; Cano ZP ; Park MG ; Yu A ; Fowler M ; Chen Z , Adv. Mater 2017, 29, 1604685.

(2). Cook SA ; Borovik AS , Acc. Chem. Res 2015, 48, 2407–2414. [PubMed: 26181849]

(3). (a)Elwell CE ; Gagnon NL ; Neisen BD ; Dhar D ; Spaeth AD ; Yee GM ; Tolman WB , Chem. Rev 2017, 117, 2059–2107; [PubMed: 28103018] (b)Suzuki M , Acc. Chem. Res 2007, 40, 609–617; [PubMed: 17559187] (c)Kim SO ; Sastri CV ; Seo MS ; Kim J ; Nam W , J. Am. Chem. Soc 2005, 127, 4178–4179. [PubMed: 15783193]

(4). Takayuki K ; Takashi F ; Ayumi T ; Mitsuru T ; Yoshihiro M ; Tomoya M , Chem. Lett 2010, 39, 136–137.

(5). Lopez N ; Graham DJ ; McGuire R ; Alliger GE ; Shao-Horn Y ; Cummins CC ; Nocera DG , Science 2012, 335, 450–453. [PubMed: 22282808]

(6). Chmielewski M ; Jurczak J , Tet. Lett 2004, 45, 6007–6010.

(7). (a)Tutusaus O ; Ni C ; Szymczak NK , J. Am. Chem. Soc 2013, 135, 3403–3406; [PubMed: 23421523] (b)Dahl EW ; Szymczak NK , Angew. Chem. Int. Ed 2016, 55, 3101–3105;(c)Tseng K-NT ; Kampf JW ; Szymczak NK , J. Am. Chem. Soc 2016, 138, 10378–10381; [PubMed: 27472301] (d)Geri JB ; Shanahan JP ; Szymczak NK , J. Am. Chem. Soc 2017, 139, 5952–5956; [PubMed: 28414226] (e)Kiernicki JJ ; Zeller M ; Szymczak NK , J. Am. Chem. Soc 2017, 139, 18194–18197; [PubMed: 29227655] (f)Dahl EW ; Dong HT ; Szymczak NK , Chem. Commun 2018, 54, 892–895.

(8). (a)MacBeth CE ; Golombek AP ; Young VG ; Yang C ; Kuczera K ; Hendrich MP ; Borovik AS , Science 2000, 289, 938–941; [PubMed: 10937994] (b)Syuhei Y ; Teppei T ; Akira W ; Yasuhiro F ; Tomohiro O ; Koichiro J ; Hideki M , Chem. Lett 2007, 36, 842–843;(c)Feng G ; Mareque-Rivas JC ; Williams NH , Chem. Commun 2006, 1845–1847;(d)Tubbs KJ ; Fuller AL ; Bennett B ; Arif AM ; Berreau LM , Inorg. Chem 2003, 42, 4790–4791; [PubMed: 12895095] (e)Hart JS ; White FJ ; Love JB , Chem. Commun 2011, 47, 5711–5713;(f)Yamaguchi S ; Nagatomo S ; Kitagawa T ; Funahashi Y ; Ozawa T ; Jitsukawa K ; Masuda H , Inorg. Chem 2003, 42, 6968–6970; [PubMed: 14577757] (g)Taguchi T ; Gupta R ; Lassalle-Kaiser B ; Boyce DW ; Yachandra VK ; Tolman WB ; Yano J ; Hendrich MP ; Borovik AS , J. Am. Chem. Soc 2012, 134, 1996–1999; [PubMed: 22233169] (h)Matson EM ; Bertke JA ; Fout AR , Inorg. Chem 2014, 53, 4450–4458; [PubMed: 24758308] (i)Ford CL ; Park YJ ; Matson EM ; Gordon Z ; Fout AR , Science 2016, 354, 741–743; [PubMed: 27846604] (j)Wallen CM ; Palantinus L ; Basca J ; Scarborough CC Angew. Chem. Int. Ed 2016, 55, 11902–11906.

(9). (a)Yamaguchi S ; Takahashi T ; Wada A ; Funahashi Y ; Ozawa T ; Jitsukawa K ; Masuda H , Chem. Lett 2007, 36, 842–843;(b)Saad FA ; Knight JC ; Kariuki BM ; Amoroso AJ , Dalton Trans 2013, 42, 14826–14835; [PubMed: 23986104] (c)Rivas JC ; Prabaharan R ; de Rosales RT ; Metteau L ; Parsons S , Dalton Trans 2004, 2800–2807; [PubMed: 15514768] (d)Syuhei Y ; Isao T ; Yoko W ; Yasuhiro F ; Koichiro J ; Hideki M , Chem. Lett 2003, 32, 406–407;(e)Wallen CM ; Bacsa J ; Scarborough CC , J. Am. Chem. Soc 2015, 137, 14606–14609. [PubMed: 26560687]

(10). (a)Forbes GC ; Kennedy AR ; Mulvey RE ; Rowlings RB ; Clegg W ; Liddle ST ; Wilson CC , Chem. Commun 2000, 1759–1760;(b)Sobota P ; Petrus R ; Zelga K ; Makolski L ; Kubicki D ; Lewiński J , Chem. Commun 2013, 49, 10477–10479.

(11). This reaction always produces (L^H)Zn(OH)(OTf) as a side-product, the relative quantity of which can be diminished during the reaction by rapidly adding cobaltocene. See supporting information.

(12). **1**^{H} was the only product observed, even when using <1 equiv N^{i}Pr$_2$Et, indicating zinc-hydroperoxide species are not accessible.

(13). Masuda and coworkers were able to spectroscopically observe a Zn(OOH) with a similar ligand framework: Wada A ; Yamaguchi S ; Jitsukawa K ; Masuda H , Angew. Chem. Int. Ed 2005, 44, 5698–5701.

(14). Other than the cobaltocene reduction and PhICl$_2$ oxidation, reactions were carried out on the benchtop with no effort to exclude air/moisture. **1**^{H} is quantitatively converted to (L^H)Zn(OH)(OTf) on exposure to 1000 fold exess of methanol or H$_2$O.

(15). Adding equimolar [Bu$_4$N][Cl] results in gradual degradation at room temperature and full degradation at 50 °C over 1 hour to unidentified species.

(16). Steiner T , Angew. Chem. Int. Ed 2002, 41, 48–76.

(17). Kiernicki JJ ; Newell BS ; Matson EM ; Anderson NH ; Fanwick PE ; Shores MP ; Bart SC , Inorg. Chem 2014, 53, 3730–3741. [PubMed: 24611564]

(18). Takamizawa S ; Nakata E.-i. ; Akatsuka T ; Kachi-Terajima C ; Miyake R , J. Am. Chem. Soc 2008, 130, 17882–17892. [PubMed: 19067574]

(19). Tao X ; Daniliuc CG ; Janka O ; Pöttgen R ; Knitsch R ; Hansen MR ; Eckert H ; Lübbesmeyer M ; Studer A ; Kehr G ; Erker G , Angew. Chem. Int. Ed 2017, 56, 16641–16644.

(20). Henthorn JT ; Agapie T , Angew. Chem. Int. Ed 2014, 53, 12893–12896.

(21). Tsurumaki E ; Sung J ; Kim D ; Osuka A , Angew. Chem. Int. Ed 2016, 55, 2596–2599.

(22). The degree of O-O activation in $\mathbf{1^H}$ is greater than terminal four-coordinate Zn-OOR examples of the tris(oxazolinyl)borate or β-diketiminate ligand frameworks, see: Mukherjee D ; Ellern A ; Sadow AD , J. Am. Chem. Soc 2012, 134, 13018–13026; [PubMed: 22839354] Xu S ; Everett WC ; Ellern A ; Windus TL ; Sadow AD , Dalton Trans 2014, 43, 14368–14376. [PubMed: 24938822] Pietrzak T ; Korzyński MD ; Justyniak I ; Zelga K ; Kornowicz A ; Ochal Z ; Lewiński J , Chem. – Eur. J 2017, 23, 7997–8005. [PubMed: 28399333]

(23). Jacobson RR ; Tyeklar Z ; Farooq A ; Karlin KD ; Liu S ; Zubieta J , J. Am. Chem. Soc 1988, 110, 3690–3692.

(24). Murthy NN ; Karlin KD , J. Chem. Soc., Chem. Commun 1993, 1236–1238.

(25). (TPA)Zn(OH) reacts with CO_2 in air to form $[(TPA)_3Zn_3(CO_3)]^{4+}$.

(26). (a)Lau N ; Ziller JW ; Borovik AS , Polyhedron 2015, 85, 777–782; [PubMed: 25419035] (b)Gordon Z ; Drummond MJ ; Matson EM ; Bogart JA ; Schelter EJ ; Lord RL ; Fout AR , Inorg. Chem 2017, 56, 4852–4863; [PubMed: 28394119] (c)Jones JR ; Ziller JW ; Borovik AS , Inorg. Chem 2017, 56, 1112–1120. [PubMed: 28094522]

(27). Hansch C ; Leo A ; Taft RW , Chem. Rev 1991, 91, 165–195.

(28). The O 22– in $\mathbf{1^{NMe2}}$ is disordered over two positions and the H-bonding interactions of the minor moiety are discussed in SI.

(29). Voltammetry of $\mathbf{1^H}$ revealed an irreversible oxidation event (E_{pa} = +1.14 V vs. Fc/Fc$^+$).

(30). Under these aqueous reaction conditions, the formation of $[(L^H)Zn(OH)]^+$ is a necessary competing reaction pathway, which diverts the $\mathbf{1^H}$ into oxidatively inert Zn(OH), and prevents a higher O_2 yield.

(31). (a)Karlin KD ; Hayes JC ; Hutchinson JP ; Zubieta J , J. Chem. Soc., Chem. Commun 1983, 376–378;(b)Pate JE ; Ross PK ; Thamann TJ ; Reed CA ; Karlin KD ; Sorrell TN ; Solomon EI , J. Am. Chem. Soc 1989, 111, 5198–5209.

(32). In our previous studies of $[(L^R)_2Cu_2O_2]^{2+}$, we noted vibrational spectroscopy did not reveal any ^{18}O active modes—this was again the case for $\mathbf{1^R}$. Raman spectroscopy revealed no changes on ^{18}O labeling, see SI.

(33). (a)Matson EM ; Park YJ ; Bertke JA ; Fout AR , Dalton Trans 2015, 44, 10377–10384; [PubMed: 25970267] (b)Reid SD ; Wilson C ; Blake AJ ; Love JB , Dalton Trans 2010, 39, 418–425; (c)Tchertanov L , Acta Crystallogr. B 1999, 55, 807–809; [PubMed: 10927421] (d)Tchertanov L , Supramol. Chem 2000, 12, 67–91;(e)Xie J ; Yikilmaz E ; Miller A-F ; Brunold TC , J. Am. Chem. Soc 2002, 124, 3769–3774. [PubMed: 11929267]

(34). In solution, these complexes exhibit C_3-symmetry and are likely rapidly interconverting between trigonal bipyramidal and octahedral via a hemilabile pyridyl arm. Variable temperature NMR (CD_2Cl_2) of $\mathbf{2^H}$ to −80 °C did not show coalescence to C_s symmetric species. For similar examples: See reference 9B and He Z ; Craig DC ; Colbran SB , J. Chem. Soc., Dalton Trans 2002, 4224–4235.

(35). Synthesis and characterization of (TPA)Zn(N$_3$)$_2$ described in supporting information.

(36). Duboc C ; Phoeung T ; Jouvenot D ; Blackman AG ; McClintock LF ; Pécaut J ; Collomb M-N ; Deronzier A , Polyhedron 2007, 26, 5243–5249.

(37). de la Cruz C ; Sheppard N , J. Mol. Struct 1990, 224, 141–161.

(38). Solution IR spectroscopy provided the same magnitude of shifts between equitorial and axial azido ligands. See supporting information.

(39). Asymmetric modes were calculated for (TPA)Zn(N$_3$)$_2$ at 2221 and 2196 cm^{-1}. The difference between the modes, 25 cm^{-1}, is in agreement with experimental, 24.9 cm^{-1}. See SI for details.

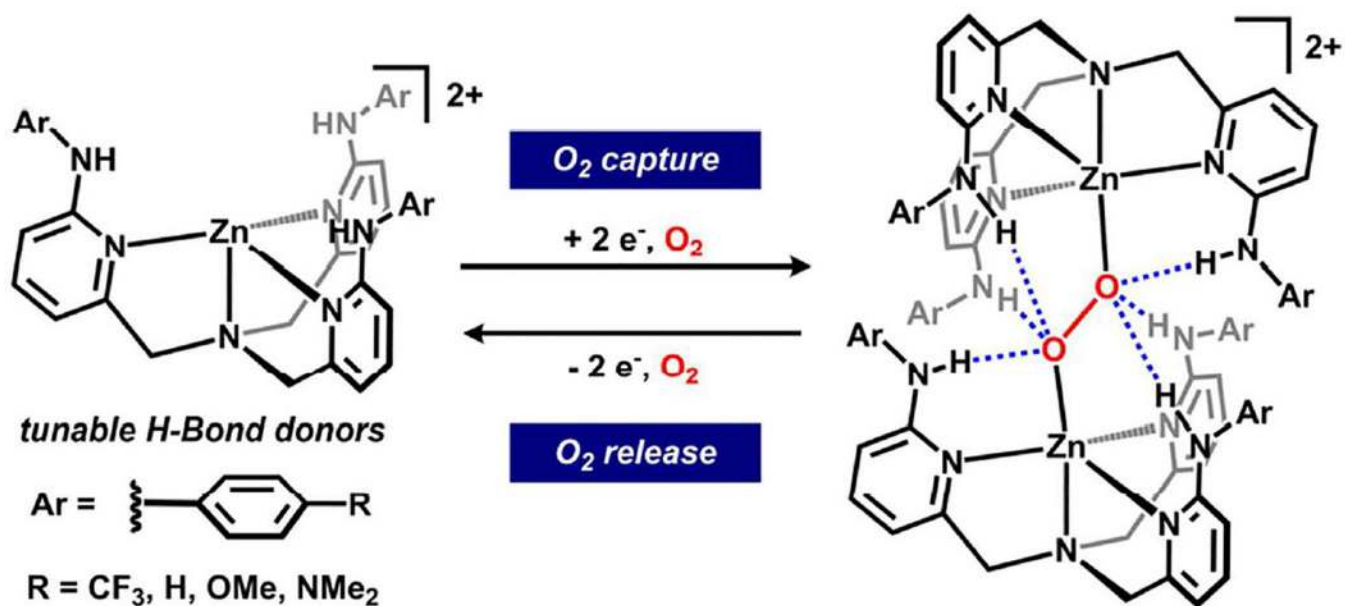(40). Moore CM ; Szymczak NK , Chem. Commun 2015, 51, 5490–5492.

Figure 1.
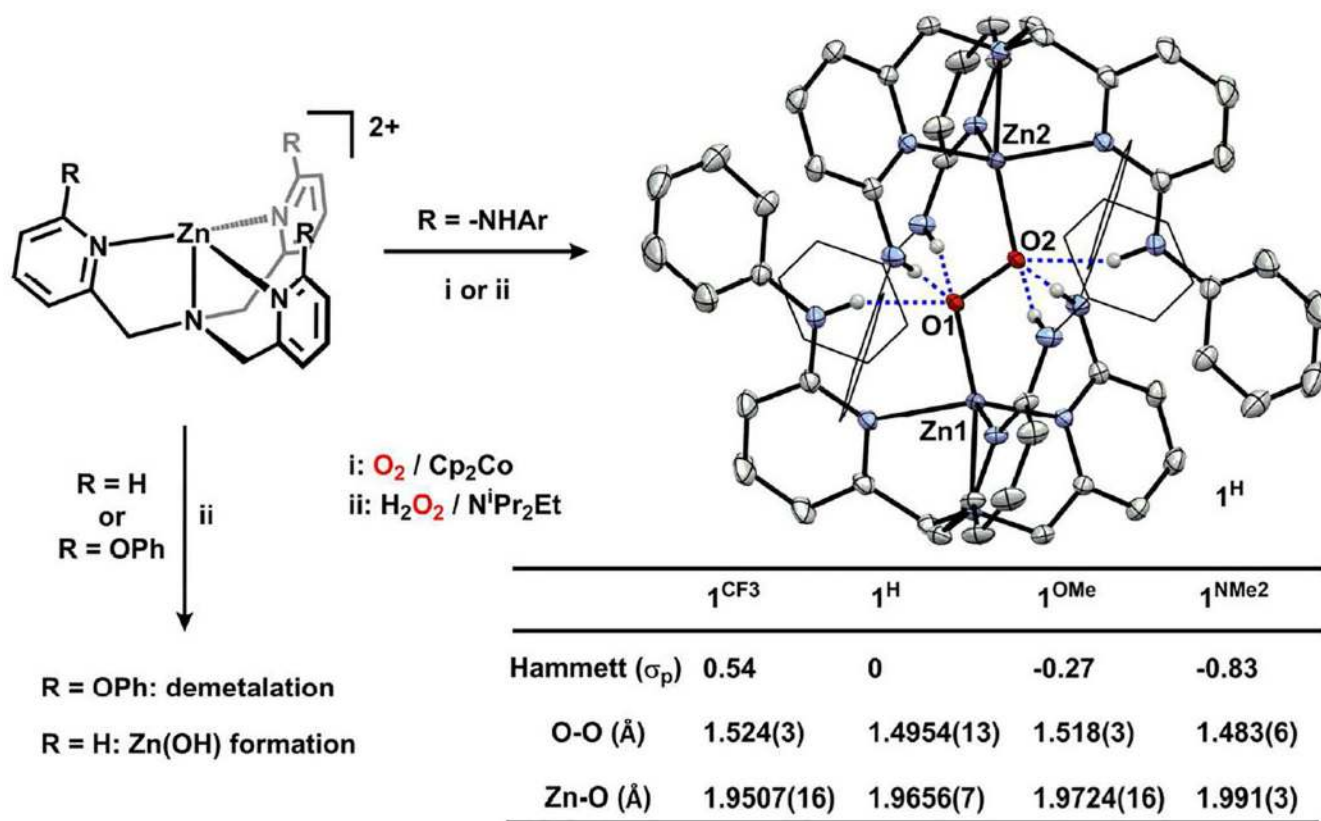Reversible O_2 capture and reduction enabled by H-bonding interactions.

Figure 2.
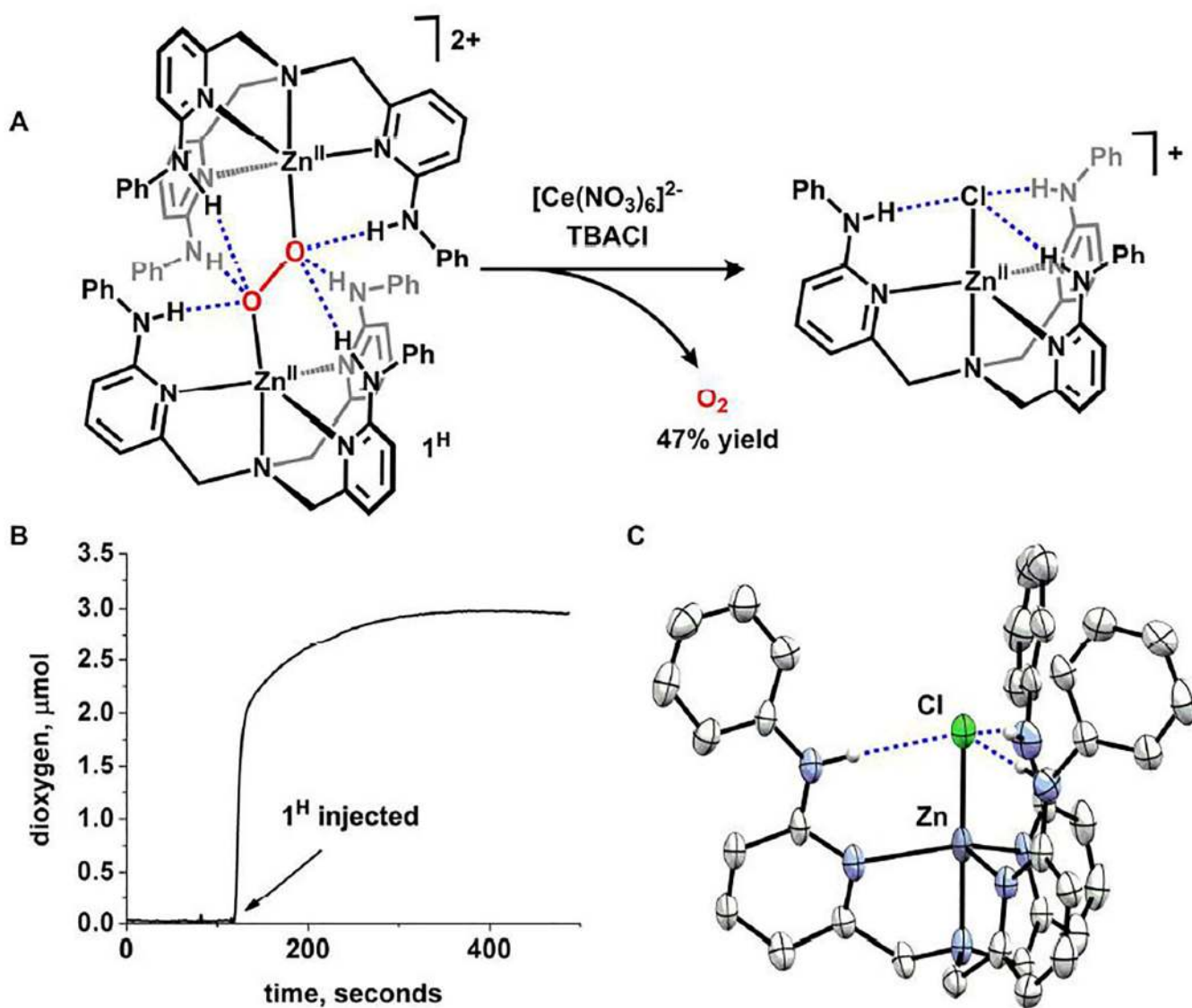Synthesis of **1^R** and molecular structure of **1^H** (50% probability ellipsoids) with bond distances of **1^R**.

	1^CF3	1^H	1^OMe	1^NMe2
Hammett (σ_p)	0.54	0	-0.27	-0.83
O-O (Å)	1.524(3)	1.4954(13)	1.518(3)	1.483(6)
Zn-O (Å)	1.9507(16)	1.9656(7)	1.9724(16)	1.991(3)

Figure 3.
A) Oxidative release of dioxygen from **1^H**. B) Dioxygen evolution trace detected by Clark electrode. C) Molecular structure of [(L^H)ZnCl]^+ (50% probability ellipsoids).
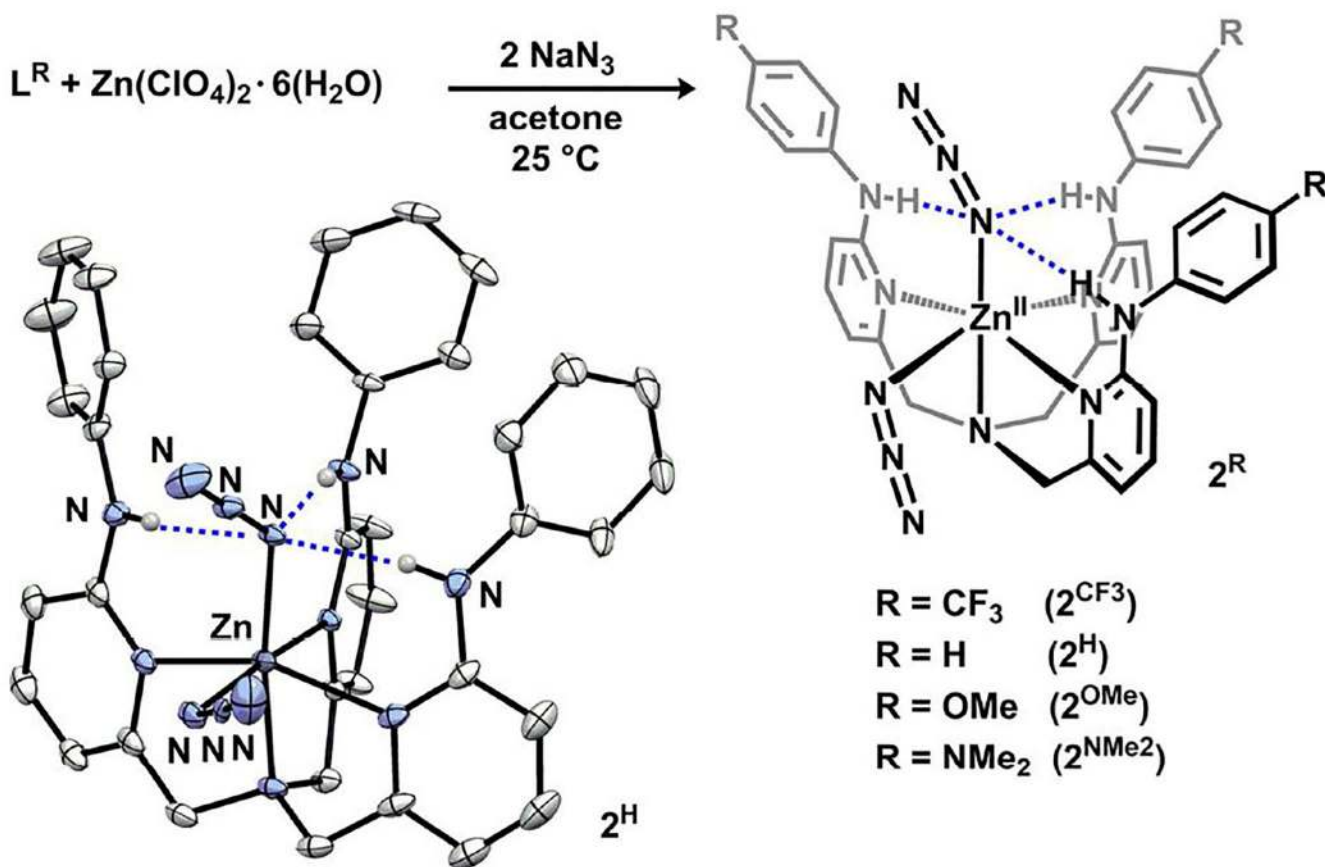
Figure 4.
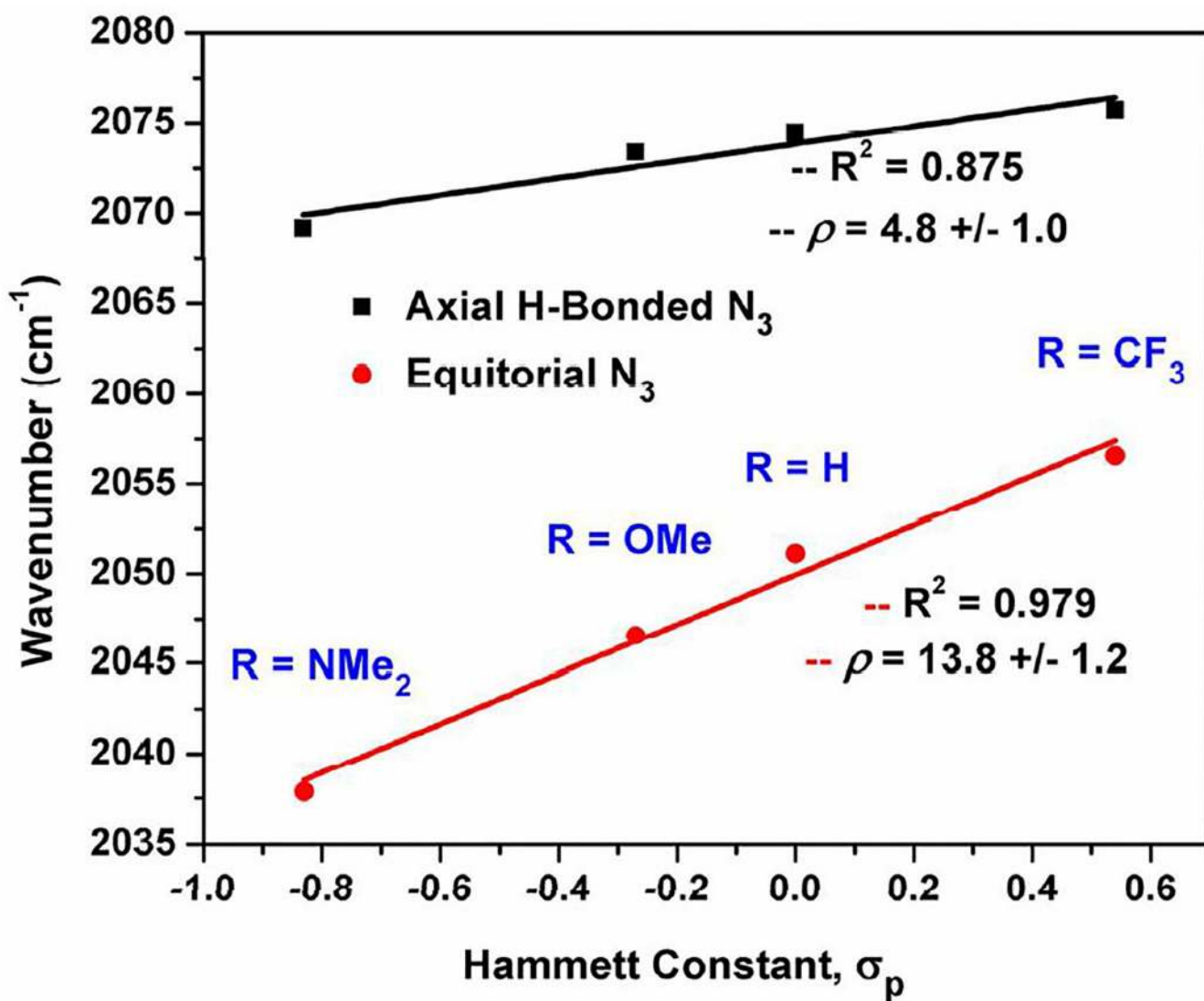Synthesis of 2^R and molecular structure of 2^H (30% probability ellipsoids).

Figure 5.
Linear free energy relationship of $\nu_{(N3)}$ (neat, ATR) and Hammett constants for $2^{\mathbf{R}}$.